

Article

Magnetic Properties of the Ferromagnetic Shape Memory Alloys $\text{Ni}_{50+x}\text{Mn}_{27-x}\text{Ga}_{23}$ in Magnetic Fields

Takuo Sakon ^{1,*}, Kohei Otsuka ¹, Junpei Matsubayashi ¹, Yuushi Watanabe ¹, Hironori Nishihara ¹, Kenta Sasaki ², Satoshi Yamashita ³, Rie Y. Umetsu ⁴, Hiroyuki Nojiri ⁴ and Takeshi Kanomata ^{5,6}

¹ Department of Mechanical and Systems Engineering, Faculty of Science and Technology, Ryukoku University, Otsu 520-2194, Japan; E-Mails: t100180@mail.ryukoku.ac.jp (K.O.); t100249@mail.ryukoku.ac.jp (J.M.); t100270@mail.ryukoku.ac.jp (Y.W.); h_nishi_hara@yahoo.co.jp (H.N.)

² Department of Mechanical Engineering, Graduate School of Engineering and Resource Science, Akita University, Akita 010-8502, Japan; E-Mail: saza6694@yahoo.co.jp

³ Faculty of Engineering, Tohoku Gakuin University, Tagajo 985-8537, Japan; E-Mail: s.y.0641247@gmail.com

⁴ Institute for Materials Research, Tohoku University, Sendai 980-8577, Japan; E-Mails: rieume@imr.tohoku.ac.jp (R.Y.U.); nojiri@imr.tohoku.ac.jp (H.N.)

⁵ Research Institute for Engineering and Technology, Tohoku Gakuin University, Tagajo 985-8537, Japan; E-Mail: kanomata@tjcc.tohoku-gakuin.ac.jp

⁶ Department of Materials Research, Graduate School of Engineering, Tohoku University, Sendai 980-8579, Japan

* Author to whom correspondence should be addressed; E-Mail: sakon@rins.ryukoku.ac.jp; Tel.: +81-77-543-7443; Fax: +81-77-543-7457.

Received: 23 February 2014; in revised form: 2 April 2014 / Accepted: 4 May 2014 /

Published: 8 May 2014

Abstract: Thermal strain, permeability, and magnetization measurements of the ferromagnetic shape memory alloys $\text{Ni}_{50+x}\text{Mn}_{27-x}\text{Ga}_{23}$ ($x = 2.0, 2.5, 2.7$) were performed. For $x = 2.7$, in which the martensite transition and the ferromagnetic transition occur at the same temperature, the martensite transition starting temperature T_{Ms} shift in magnetic fields around a zero magnetic field was estimated to be $dT_{\text{Ms}}/dB = 1.1 \pm 0.2$ K/T, thus indicating that magnetic fields influences martensite transition. We discussed the itinerant electron magnetism of $x = 2.0$ and 2.5 . As for $x = 2.5$, the M^4 vs. B/M plot crosses the origin of the coordinate axis at the Curie temperature, and the plot indicates a good linear relation

behavior around the Curie temperature. The result is in agreement with the theory by Takahashi, concerning itinerant electron ferromagnets.

Keywords: shape memory alloys; thermal strain; magnetization; magnetic properties; magnetic field; itinerant electron ferromagnet

1. Introduction

Ferromagnetic shape memory alloys have been extensively studied as potential candidates for smart materials. Among these alloys, Ni₂MnGa is the most familiar alloy [1]. It has a cubic $L2_1$ Heusler structure (space group $Fm\bar{3}m$) with the lattice parameter $a = 5.825 \text{ \AA}$ at room temperature, and it orders ferromagnetically at the Curie temperature $T_C \approx 365 \text{ K}$ [2,3]. Upon cooling from room temperature, a martensite transition occurs at the martensite transition temperature $T_M \approx 200 \text{ K}$. Below T_M , a superstructure forms because of lattice modulation [4,5]. For Ni-Mn-Ga Heusler alloys, the T_M can vary from 200 to 330 K by nonstoichiometrically changing the concentration of composite elements.

Several studies on Ni-Mn-Ga alloys address the martensite transition and the correlation between magnetism and crystallographic structures [6–18]. Ma *et al.* [7] studied the crystallography of Ni_{50+x}Mn₂₅Ga_{25-x} alloys ($2 \leq x \leq 11$) by powder X-ray diffraction and optical microspectroscopy. In the martensite phase, typical microstructures were observed for $x < 7$. The martensite variants exhibit configurations typical of self-accommodation arrangements. The TEM image of Ni₅₄Mn₂₅Ga₂₁ indicates that the typical width of a variant is about 1 μm .

Umetsu *et al.* [19] made a phase diagram of Ni_{50+x}Mn_{27-x}Ga₂₃ alloys ($-25 \leq x \leq 6$). The martensite transition temperature T_M and the ferromagnetic transition temperature (Curie temperature) T_C cross over at around $x = 2.5$. The martensite transition temperature of Ni_{50+x}Mn_{27-x}Ga₂₃ is higher than that of the stoichiometric composition. This property is very useful from the viewpoint of developing commercial applications.

The interaction between magnetism and crystallographic rearrangements was discussed in references [1,8,17,18]. Murray *et al.* [18] studied polycrystalline Ni-Mn-Ga alloys. The magnetization step at T_M is also observed. This is a reflection of the magnetic anisotropy in the tetragonal martensite phase. In the martensite phase, a strong magnetic anisotropy exists. Under these circumstances, the magnetization that reflects the percentage of magnetic moments parallel to the magnetic field is smaller than that of the austenite phase, where the magnetic anisotropy is not strong in the weak magnetic field. Therefore, the magnetization step is observed at T_M .

NMR experiments indicate Mn-Mn indirect exchange via the faults in Mn-Ga layers interchange, which are caused by excessive amounts of Ga [13]. This result indicates that the exchange interaction between Mn-Mn magnetic moments is sensitive to lattice transformation: during such a transformation, the magnetism changes from that of a soft magnet in the austenite phase to that of a hard magnet in the martensite phase; this is due to higher magnetic anisotropy. Dai *et al.* [20] reported this softening of the lattice; they did so by measuring the elastic constants of a Ni_{0.50}Mn_{0.284}Ga_{0.216} single crystal using the ultrasonic continuous-wave method. C_{11} , C_{33} , C_{66} and C_{44} modes were investigated; every mode

indicated an abrupt softening around T_M . This lattice softening appears to be affected by the abrupt expansion just above T_M when cooling from the austenite phase.

Takahashi proposed a spin fluctuation theory of itinerant electron magnetism [21,22]. The induced magnetization M is written as the formula of

$$\left(\frac{M}{M_S}\right)^4 = 1.20 \times 10^6 \frac{T_C^2}{T_A^3 p_S^4} \cdot \frac{H}{M} \quad (1)$$

where $M_S = N_0 \mu_B p_S$ is the spontaneous magnetization in the ground state; N_0 is the molecular number; $p_S = gS$, where g is the g-factor and S is a spin; T_A is the spin fluctuation parameter. Nishihara *et al.* [23] measured the magnetization of Ni and Ni₂MnGa. Good linearity is observed in the M^4 vs. H/M plot at the Curie temperature for Ni. This result indicates that the critical index δ (defined as $H \propto M^\delta$) is 5.0.

In this study, we focused on the physical effects of magnetic fields. By using polycrystalline samples, it was possible for us to provide information concerning the easy axis of magnetization in a martensite structure; we made temperature-dependent strain measurements under constant magnetic fields. In this paper, permeability, thermal strain, and magnetization measurements were performed for polycrystalline Ni_{50+x}Mn_{27-x}Ga₂₃ ($x = 2.5, 2.7$) in magnetic fields (B). Thermal strain and magnetization results of Ni₅₂Mn₂₅Ga₂₃ ($x = 2.0$) were used for discussing the magnetic field dependence of the martensite transition temperature and magnetization [24]. The results of thermal strain in a magnetic field and magnetic-field-induced strain yield information about the twin boundary motion in the fields. The experimental results were compared with those of other Ni-Mn-Ga single crystalline or polycrystalline alloys, and correlations between magnetism and martensite transition were found. Itinerant magnetism is also discussed, based upon the results of the magnetic field dependence of the magnetization and compared with the predictions of Takahashi's theory [21,22].

The martensite transition temperature T_M and reverse martensite phase transition T_R are used when these are quoted from the references. To define these temperatures clearly, we used T_M and T_R as the martensite transition starting temperature T_{Ms} and the reverse martensite temperature finishing temperature T_{Rf} in our research results.

2. Experimental Procedures

The Ni_{50+x}Mn_{27-x}Ga₂₃ ($x = 2.5, 2.7$) alloys were prepared by arc melting 99.99% pure Ni, 99.99% pure Mn, and 99.9999% pure Ga in an argon atmosphere. To obtain homogenized samples, the reaction products were sealed in double-evacuated silica tubes, and then annealed at 1123 K for 3 days and quenched in cold water. The obtained samples were polycrystalline. From X-ray powder diffraction, the monoclinic $6M$ phase martensite structure and the $D0_{22}$ tetragonal structure were mixed at 298 K. The size of the sample was 2.0 mm \times 2.0 mm \times 4.0 mm.

The measurements in this study were performed at atmospheric pressure ($P = 0.10$ MPa). Thermal strain measurements were performed using strain gauges (Kyowa Dengyo Co., Ltd., Chofu, Japan). The electrical resistivity of the strain gauges was measured by the four-probe method. The strain gauge was fixed parallel to the longitudinal axis of the sample.

Thermal strain measurements were performed using a 10 T helium-free cryo-cooled superconducting magnet at the High Field Laboratory for Superconducting Materials, Institute for Materials Research,

Tohoku University. The magnetic field was applied along the sample's longitudinal axis. The thermal strain is denoted by the reference strain at 360 K.

Magnetization measurements in a steady field at 5 K and temperature dependence of the magnetization at 0.10 T were performed using a SQUID magnetometer installed at Ryukoku University. As for $x = 2.7$, the high temperature magnetization between 320 K and 370 K were performed using a home-made magnetometer within a weak AC fields (with the frequency $f = 73$ Hz and the maximum field $B_{\max} = 0.0050$ T, which has a compensating high homogeneity magnetic field. AC fields were applied along the sample's longitudinal axis.), using an AC wave generator WF 1945B (NF Co., Ltd., Yokohama, Japan) and an audio amp PM17 (Marantz Co. Ltd., Kawasaki, Japan). The magnet was the same magnet with the thermal strain measurements. Pulsed magnetization measurements were performed using a Bitter-type water-cooled pulsed magnet (inner bore: 26 mm; total length: 200 mm) in a pulsed magnetic field at Ryukoku University. The magnetic field was applied along the sample's longitudinal axis. The values of magnetization were corrected using the values of spontaneous magnetization for 99.99% pure Ni. The magnetic permeability measurements were performed in AC fields, which is as same as the AC magnetometer. Thermal experiments were carried out by means of DSC, using a rate of 10 K/min.

3. Results and Discussion

3.1. Magnetic Properties of $Ni_{52.5}Mn_{24.5}Ga_{23}$ ($x = 2.5$)

Figure 1a shows the temperature dependence of permeability. When heating from 300 K, permeability increases gradually. As shown in Figure 1a, permeability increases above 343 K and suddenly decreases around 350 K. When cooling from a high temperature, permeability shows a sudden increase at 355 K and decreases below 342 K. The sudden changes in permeability indicate that the ferromagnetic transition occurs around 350 K. The temperature dependence of permeability for $Ni_{52.5}Mn_{24.5}Ga_{23}$ is similar to that of $Ni_{52}Mn_{12.5}Fe_{12.5}Ga_{23}$'s, which shows a transition of a ferromagnetic–martensite (Ferro–M) phase to a ferromagnetic–austenite (Ferro–A) phase [25]. The step above 343 K (heating process) and below 342 K (cooling process) reflects stronger magnetic anisotropy in the tetragonal martensite phase, compared with that in the cubic austenite phase [8,18,24].

Polycrystalline $Ni_{49.5}Mn_{28.5}Ga_{22}$, $Ni_{50}Mn_{28}Ga_{22}$, and $Ni_{52}Mn_{12.5}Fe_{12.5}Ga_{23}$ alloys also indicate the magnetization (or permeability) step at T_M [9,18,26] below the field of 10 mT. Figure 1b indicates the temperature dependence of the differential of permeability $d\mu/dT$. The martensite transition starting temperature T_{Ms} and reverse martensite finishing temperature T_{Rf} , which correspond to the characteristic temperature of martensite transition for thermal strain shown in Figure 2, are indicated by arrows.

Figure 2 shows the linear thermal strain of $Ni_{52.5}Mn_{24.5}Ga_{23}$. B means magnetic field and the unit is T (tesla). B is equal to $\mu_0 H$, where μ_0 is the absolute permeability of a vacuum; the unit of H is A/m. At zero magnetic fields, the memory strain was observed, as polycrystalline $Ni_{53.6}Mn_{27.1}Ga_{19.3}$ [10]. When heating from 300 K, a slight strain was observed, first at zero magnetic fields. Above 342 K, a sharp strain is observed. The results of previous studies [6,7] suggest that this is because of the reverse martensite transition $T_{Rf} = 347$ K, which is denoted by an arrow. When cooling from 360 K, a sudden

decrease is observed at 341 K. The martensite transition starting temperature T_{Ms} is 341 K, defined as the midpoint temperature of the transition. The permeability at the Ferro–M phase is very low compared with that of the Ferro–A phase. The results of permeability and linear strain measurements indicate that the region above T_{Ms} is a Ferro–A phase and that below T_{Ms} is a Ferro–M phase. The permeability measurement results indicate that the ferromagnetic transition from the paramagnetic–austenite (Para–A) phase to the Ferro–A phase occurs around $T_C = 350$ K (see Figure 1a). At zero magnetic fields, and in magnetic fields, there is no visible anomaly around T_C . When cooling from 360 K, the thermal strain also shows a peak at 336 K. This may be attributed to the intermingling of the $L2_1$ austenite lattices and the $6M$ martensite lattices at the martensite transition. A sequential phenomenon is observed in single crystalline $Ni_{2.19}Mn_{0.81}Ga$ [20]. The thermal strain shows an anomaly around $T_1 = 323$ K and $T_2 = 313$ K. The reason of this anomaly is open question at the present time. The contraction at T_{Ms} under zero field is about 0.8×10^{-3} (0.08%). As for other Heusler alloys, $Ni_{52}Mn_{12.5}Fe_{12.5}Ga_{23}$ and $Ni_2Mn_{0.75}Cu_{0.25}Ga$, the contraction occurs at the martensite temperature [26]. The strain at T_M of polycrystalline $Ni_{52}Mn_{12.5}Fe_{12.5}Ga_{23}$ was estimated as 0.14% contraction. This value is larger than that of $Ni_{52.5}Mn_{24.5}Ga_{23}$. After zero field measurements of the linear strain, measurements in magnetic fields from 3 T to 10 T were performed. The strains at T_{Ms} under the magnetic field were estimated as 0.08% contraction, which is the same as that at zero magnetic field (0.08%).

Figure 1. (a) Temperature dependence of the magnetic permeability μ of $Ni_{52.5}Mn_{24.5}Ga_{23}$ in AC fields with $f = 73$ Hz and $B_{max} = 0.0050$ T. The origin of the vertical axis is the reference point when the sample is empty in the pickup coil of the magnetic permeability measurement system; (b) the $d\mu/dT$ vs. T . T_{Ms} and T_{Rf} , which correspond to the characteristic temperature of martensite transition for thermal strain shown in Figure 2, are indicated by arrows.

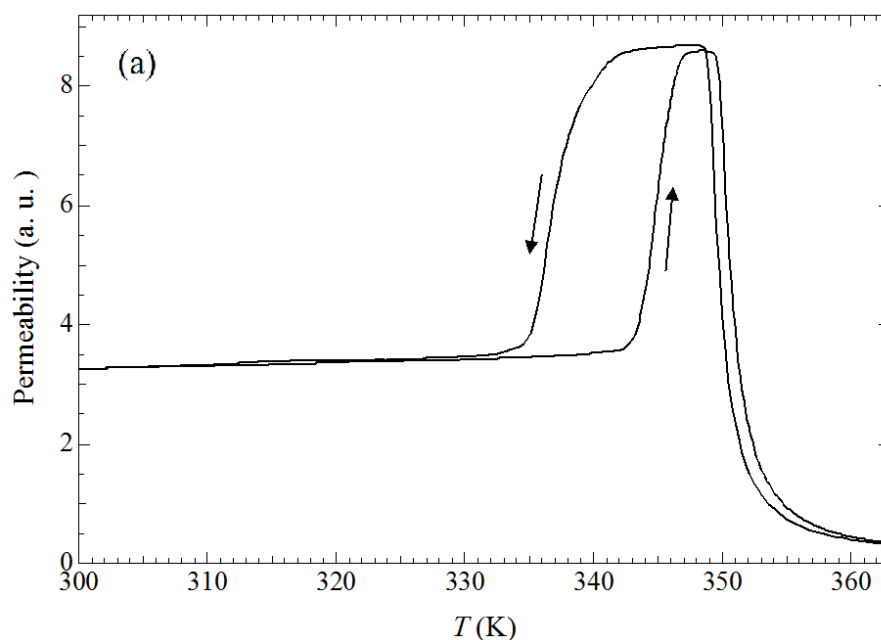


Figure 1. Cont.

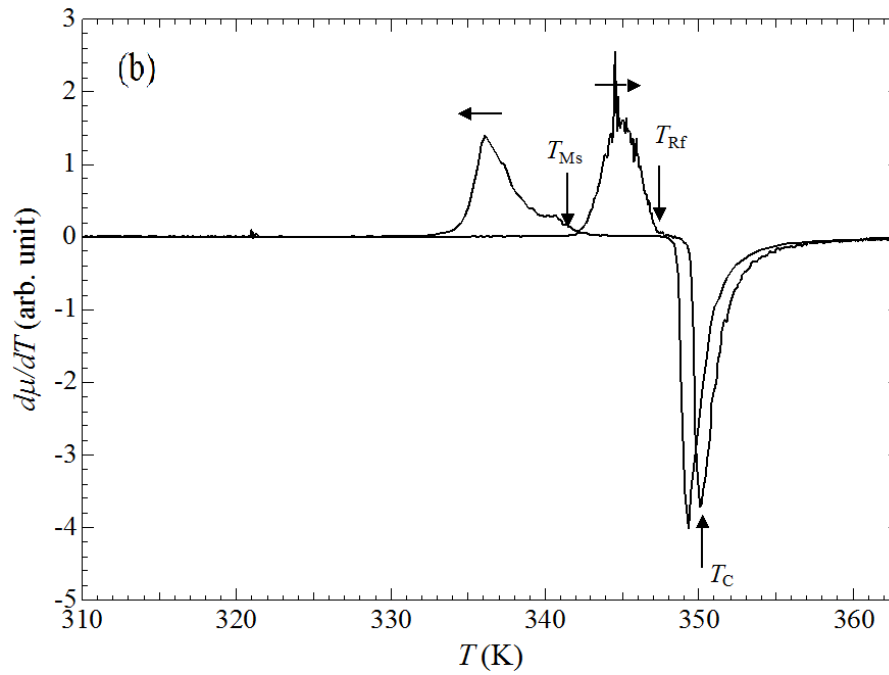


Figure 2. Temperature dependence of the linear thermal strain of Ni_{52.5}Mn_{24.5}Ga₂₃ in static magnetic fields.

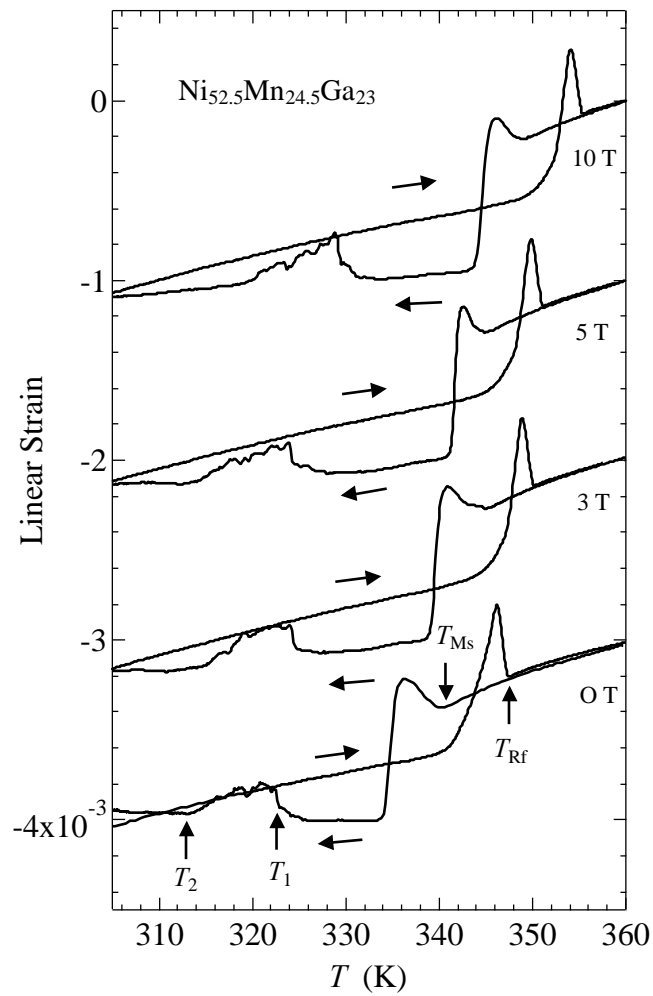


Figure 3 shows the magnetic-field-induced strain at 300 K (Ferro–M phase) in a static magnetic field. When increasing the magnetic field from zero field, a sudden contraction occurs up to 1 T. Above 1 T, a gradual contraction is observed. When decreasing the magnetic field from 10 T, a modicum of strain occurs. Below 1 T, a sudden strain is observed. The magnetic-field-induced strain at 10 T is -50 ppm or -0.005% .

The reasons that magnetic-field-induced strain is smaller than the strain at T_M , in the linear strain measurements, were elucidated in references [18,24,27].

On heating from the martensite phase, an abrupt increase occurred in the field-induced strain around T_M . They suggest that this is caused by lattice softening near T_M . As for the thermal strain of $\text{Ni}_{52.5}\text{Mn}_{24.5}\text{Ga}_{23}$, shown in Figure 2, peaks appear for both T_{Ms} and T_{Rf} in zero field and all values of the magnetic field. The peak at T_{Rf} , which is associated with heating, is larger than the one at T_{Ms} , which is associated with cooling. These peaks indicate that the lattice expands abruptly. The ultrasonic continuous-wave measurements by Dai *et al.* [20] indicated abrupt softening around T_M . This lattice softening appears to be affected by the abrupt expansion just above T_M or T_R , when cooling or heating from or to the austenite phase, respectively.

Figure 3. Magnetostriction of $\text{Ni}_{52.5}\text{Mn}_{24.5}\text{Ga}_{23}$ at 300 K in a static magnetic field of up to 10 T.

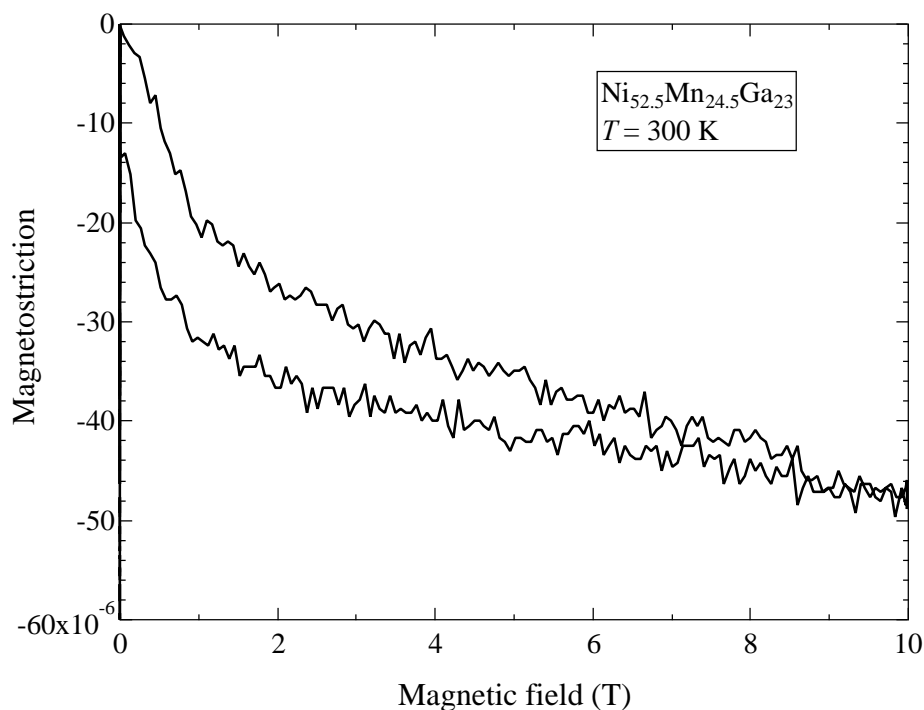


Figure 4 shows the magnetic phase diagram of $\text{Ni}_{52.5}\text{Mn}_{24.5}\text{Ga}_{23}$. With increasing field, T_{Ms} and T_{Rf} gradually increase. The shifts in T_{Ms} and T_{Rf} around zero magnetic field are estimated as $dT_{Ms}/dB = 0.9 \pm 0.2$ K/T and $dT_{Rf}/dB = 0.8 \pm 0.2$ K/T, which is larger than those of the $\text{Ni}_{52}\text{Mn}_{12.5}\text{Fe}_{12.5}\text{Ga}_{23}$ alloy's ($dT_M/dB = 0.5$ K/T) [26]. In Section 3.2, we will discuss the shifts in T_{Ms} and T_{Rf} under magnetic fields.

Figure 4. Magnetic phase diagram of $\text{Ni}_{52.5}\text{Mn}_{24.5}\text{Ga}_{23}$. Filled triangles indicate the martensite transition start temperature T_{Ms} . Filled circles indicate the reverse martensite finishing temperature T_{Rf} .

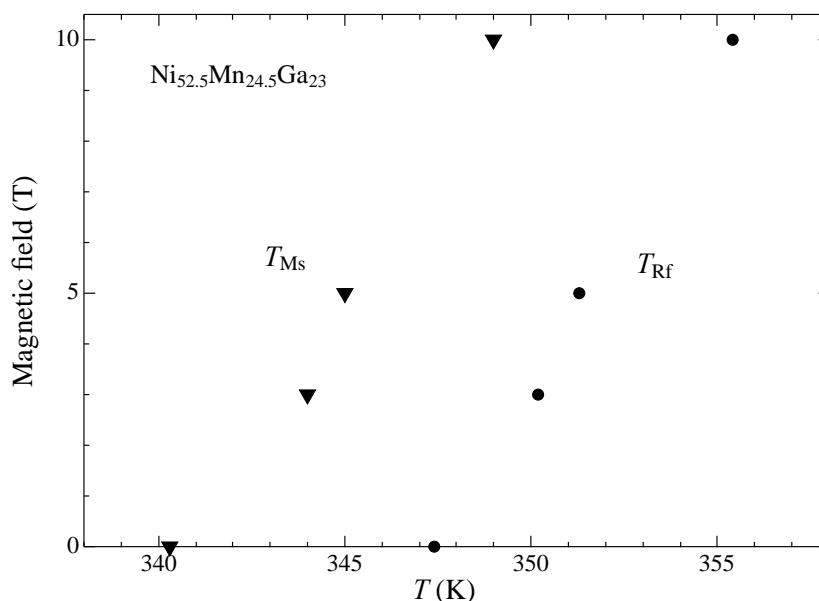


Figure 5a shows the magnetization curves of $\text{Ni}_{52.5}\text{Mn}_{24.5}\text{Ga}_{23}$ at 5 K in a static magnetic field measured by a SQUID magnetometer. The unit of magnetization M is Am^2/kg in the SI unit system or emu/g in the CGS unit system (both have identical numerical values). The saturation magnetization was $79.6 \text{ Am}^2/\text{kg}$. The spontaneous magnetization was $77.7 \text{ Am}^2/\text{kg}$ (which was derived from the Arrott plot) as shown in Figure 5b. This spontaneous magnetization value is equal to a magnetic moment of $3.35 \mu_{\text{B}}/\text{f.u.}$ This absolute value corresponds to $3.75 \mu_{\text{B}}/\text{Mn}$. The Mn magnetic moment of $3.75 \mu_{\text{B}}$ is comparable to the magnetic moment of Mn on the B site, which is approximately $3.58 \mu_{\text{B}}/\text{Mn}$ (as obtained from the powder neutron scattering experiments performed by Ahuja *et al.* [28]). Detailed expressions about the magnetic moments of $\text{Ni}_{50+x}\text{Mn}_{27-x}\text{Ga}_{23}$ alloys ($-25 \leq x \leq 6$) were described by Umetsu *et al.* [19].

Figure 5c shows the temperature dependence of magnetization at 0.10 T. During the heating process, a decrease in magnetization occurred between 350 and 360 K, which corresponds to the magnetic transition, as shown in Figure 1a. Notably, this abrupt decrease in the M - T curve at T_{Ms} is different from that of usual ferromagnets. The assumed reason is that martensite transition occurs just below the Curie temperature T_{C} for $\text{Ni}_{52.5}\text{Mn}_{24.5}\text{Ga}_{23}$. For $x = 5$, the M - T curve shows a gradual decrease at T_{Ms} during the heating process. At this composition, the magnetic transition occurs in the martensite phase.

Figure 6a shows the magnetization curves of $\text{Ni}_{52.5}\text{Mn}_{24.5}\text{Ga}_{23}$ in a pulsed magnetic field up to 2.2 T. The M - B curves were measured from low temperatures. The hysteresis of the M - B curve is considerably small. The magnetocaloric effects in other magnetic materials were also reported; for example, Levitin *et al.* [29] reported for $\text{Gd}_3\text{Ga}_5\text{O}_{12}$. They performed magnetization measurements at an initial temperature of 4.2 K, where the magnetic contribution to heat capacity is comparable to that of the lattice heat capacity. In our experiment, the temperature change of the sample due to the magnetocaloric effect is considered to be within 1 K. This is because these experiments were performed around room temperature, where the lattice heat capacity is much larger than the heating

or cooling power of the magnetocaloric effect. Moreover, M - B curves in Figure 6a show rather small hysteresis, which indicates that the magnetizations have been measured under a static temperature condition.

Figure 5. (a) Magnetization of $\text{Ni}_{52.5}\text{Mn}_{24.5}\text{Ga}_{23}$ in a static magnetic field; (b) Arrott plot of magnetization at 5 K; (c) temperature dependence of magnetization at 0.10 T.

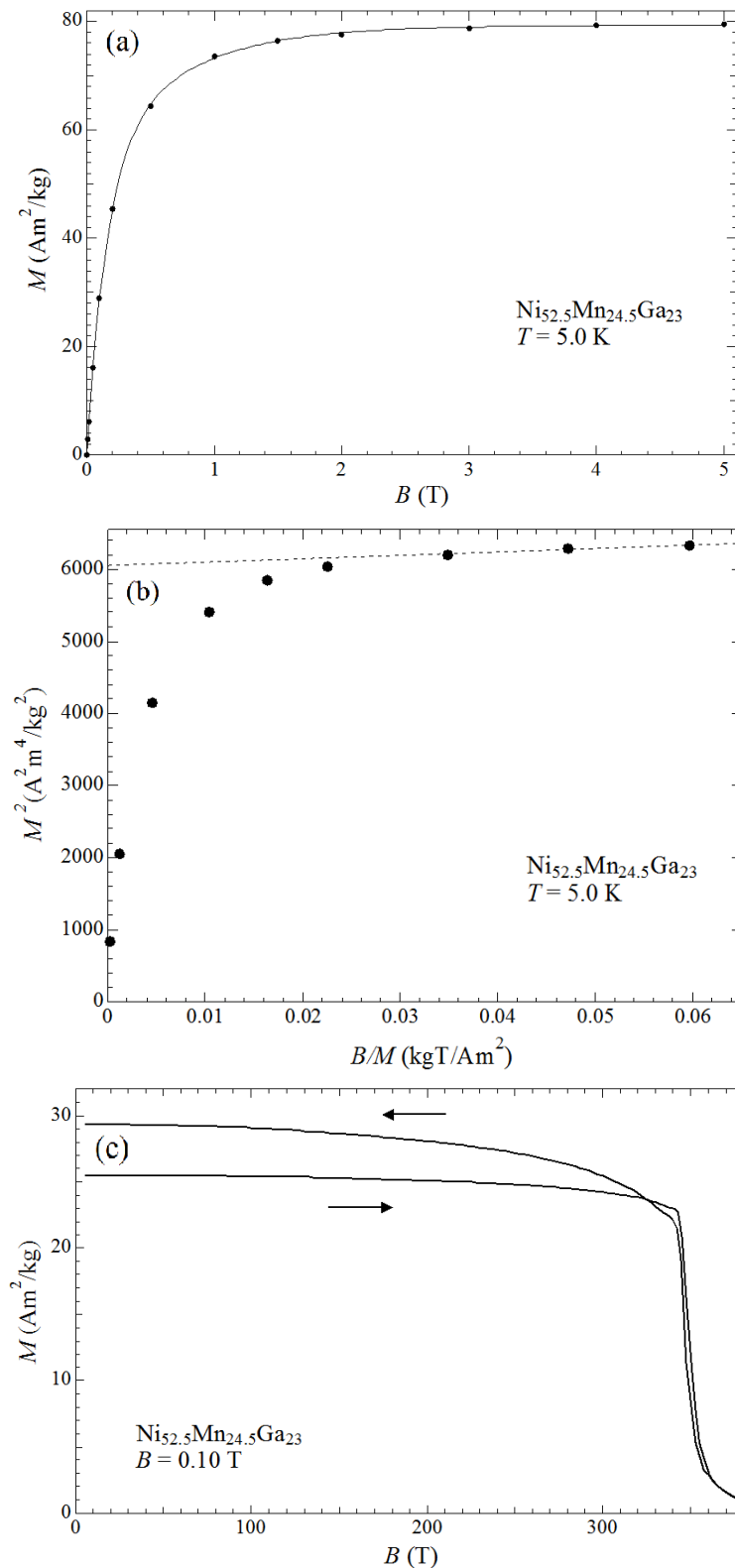
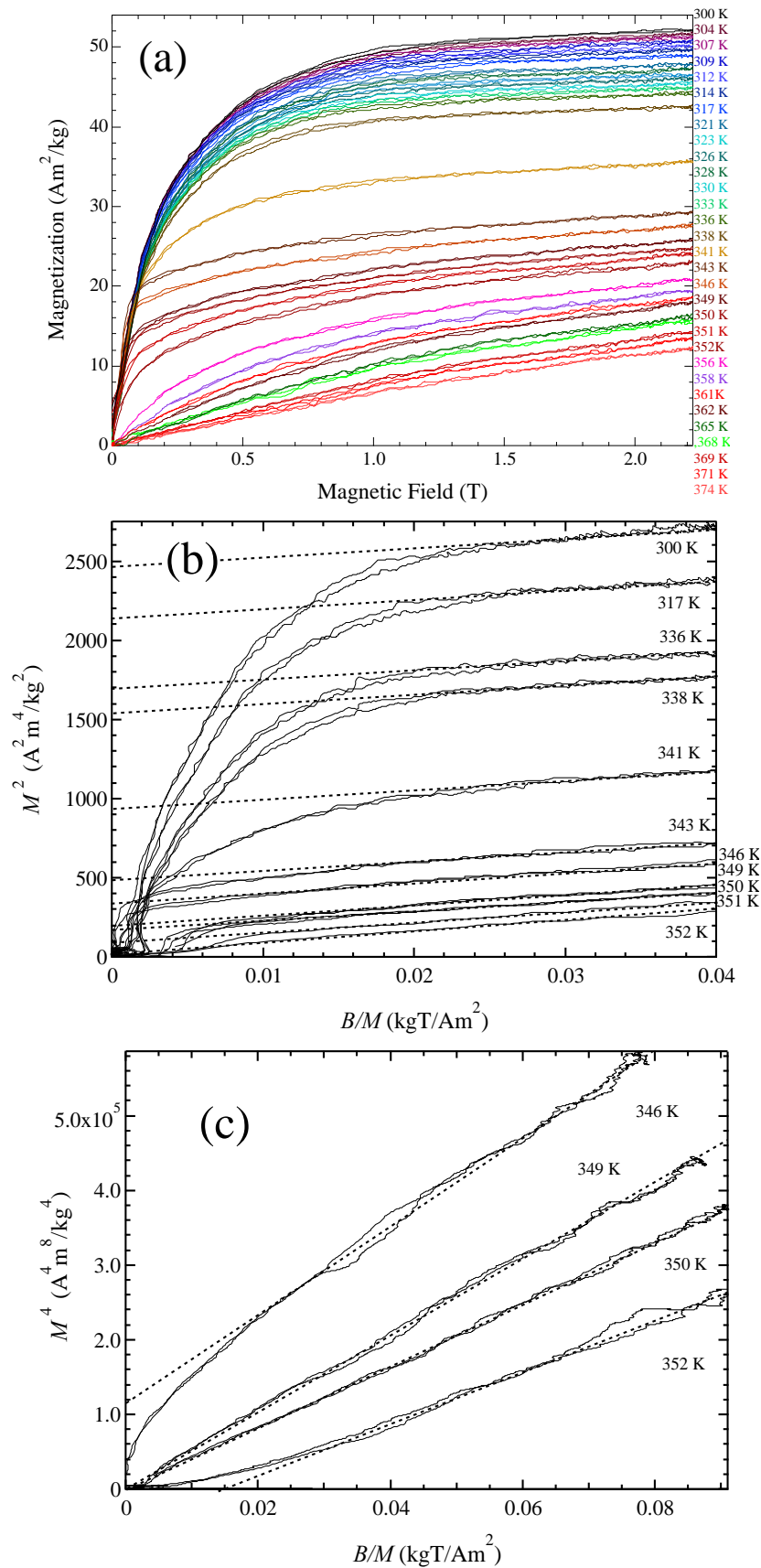


Figure 6. (a) Magnetization of $\text{Ni}_{52.5}\text{Mn}_{24.5}\text{Ga}_{23}$ in a pulsed magnetic field up to 2.2 T; (b) Arrott plot of the magnetization of $\text{Ni}_{52.5}\text{Mn}_{24.5}\text{Ga}_{23}$. Dotted straight lines are extrapolated lines; (c) M^4 vs. B/M plot for $\text{Ni}_{52.5}\text{Mn}_{24.5}\text{Ga}_{23}$. Dotted straight lines are extrapolated lines.



The M - B curves show ferromagnetic behavior below 350 K. Clearly, the field dependence of magnetization at the Ferro–A phase above $T_{Rf} = 347$ K is different from that of the Ferro–M phase around T_{Rf} . At the Ferro–M phase, magnetization increases with magnetic fields. On the other hand, at the Ferro–A phase between 334 and 356 K, a sudden increase in magnetization occurs between 0 and 0.1 T.

Figure 6b shows the Arrott plot of $\text{Ni}_{52.5}\text{Mn}_{24.5}\text{Ga}_{23}$. This plot was also used for estimating the spontaneous magnetization to discuss the dT_M/dB by means of the Clausius-Clapeyron relation. The spontaneous magnetization in $\text{Ni}_{52.5}\text{Mn}_{24.5}\text{Ga}_{23}$ at 338 K, just below T_R is $39.1 \text{ Am}^2/\text{kg}$, which was obtained by the Arrott plot in Figure 6b. When using this value as the M_S , the magnetocrystalline anisotropy energy in the martensite phase of $\text{Ni}_{52.5}\text{Mn}_{24.5}\text{Ga}_{23}$ is $M_S B_S/2 = K_U = 1.7 \times 10^5 \text{ J/m}^3$, which is on the same order as that in the martensite phase of Ni_2MnGa . These magnetic properties were also shown for $\text{Ni}_{51.9}\text{Mn}_{23.2}\text{Ga}_{24.9}$ [11], $\text{Ni}_{49.5}\text{Mn}_{25.4}\text{Ga}_{25.1}$ [12], and $\text{Ni}_{54}\text{Mn}_{21}\text{Ga}_{25}$ [13].

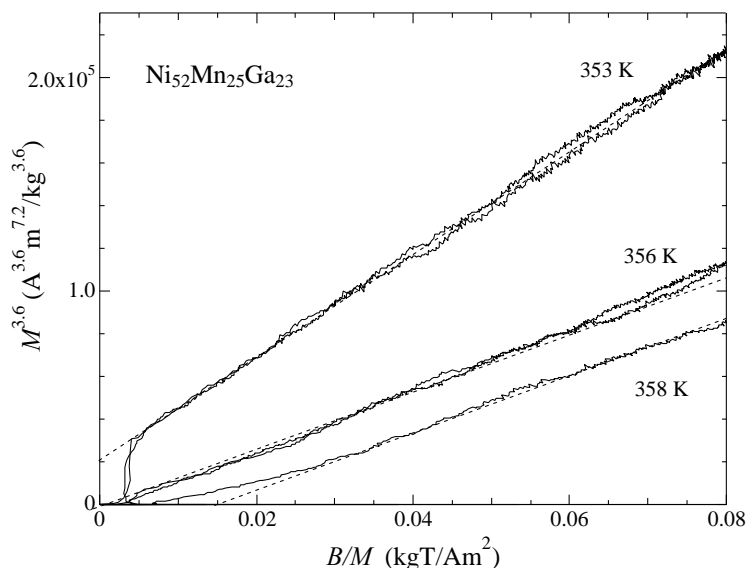
At large B/M values, the M^2 vs. B/M plot seems to show a linear relation. However, around T_C , the M^2 vs. B/M plot strays out from a linear relation at low B/M values. Therefore, we made an attempt of other plot.

Figure 6c shows the M^4 vs. B/M plots. The M^4 vs. B/M plot indicates a good linear relation around the Curie temperature $T_C = 350$ K. The critical index δ for M^δ vs. B is 5.0. The result is in agreement with the theory by Takahashi for weak itinerant electron ferromagnets [21,22].

The $M^{3.6}$ vs. B/M plot for $\text{Ni}_{52}\text{Mn}_{25}\text{Ga}_{23}$ is shown in Figure 7. The magnetic properties were reported in our former research [24]. This plot indicates a good linear relation around the Curie temperature $T_C = 356$ K. The critical index δ is 4.6. Nishihara *et al.* [23] investigated the magnetic field dependence of the magnetization of Ni_2MnGa around $T_C = 363$ K. The critical index δ is 4.77. As for Takahashi theory's formula as shown in Equation (1), the critical index δ is 5.0. Therefore, we analyze of the characteristic temperature T_A for $\text{Ni}_{52.5}\text{Mn}_{24.5}\text{Ga}_{23}$.

From the magnetic moment $3.75 \mu_B/\text{Mn}$ obtained from our magnetization measurement and the gradient of M^4 vs. B/M in Figure 6c, we calculated the characteristic temperature T_A as 1.06×10^4 K. This value is comparable to the value of Co_2CrGa (1.0×10^4 K) [30] and Ni (1.76×10^4 K) [21]. These results reflect the nature of itinerant magnetism for $\text{Ni}_{52.5}\text{Mn}_{24.5}\text{Ga}_{23}$.

Figure 7. $M^{3.6}$ vs. B/M plot for $\text{Ni}_{52}\text{Mn}_{25}\text{Ga}_{23}$. Dotted straight lines are extrapolated lines.



3.2. Magnetic Properties of $Ni_{52.7}Mn_{24.3}Ga_{23}$ ($x = 2.7$)

$Ni_{52.7}Mn_{24.3}Ga_{23}$ is an alloy in which the martensite transition and ferromagnetic transition occurred at the same temperature [19]. Figure 8 shows the temperature dependence of the linear thermal strain of $Ni_{52.7}Mn_{24.3}Ga_{23}$ in static magnetic fields, parallel to the longitudinal direction of the sample. With increasing field, T_{Ms} and T_{Rf} gradually increased. The shifts in T_{Ms} and T_{Rf} around zero magnetic field are estimated as dT_{Ms}/dB and dT_{Rf}/dB as 1.1 ± 0.2 K/T. Thermal strain results indicate that, with cooling from austenite phase, the elongation occurred at T_{Ms} . The same phenomenon was observed in the $Ni_{2.19}Mn_{0.81}Ga$ and $Ni_{2.20}Mn_{0.80}Ga$ polycrystalline samples. It should be noted that these alloys also show the martensitic and ferromagnetic transitions at the same temperature [31]. For the temperature dependence of the linear thermal strain of $Ni_{52.7}Mn_{24.3}Ga_{23}$ perpendicular to the longitudinal direction, contraction occurred at T_{Ms} with cooling from austenite phase. As for the lattice parameters of $Ni_{52.7}Mn_{24.3}Ga_{23}$, martensite phase c -axis parameter is 11% larger than austenite phase a -axis parameter, and, martensite phase a -axis parameter is 6% smaller than austenite phase a -axis parameter [19]. Therefore, it is conceivable that the difference of these linear strains parallel or perpendicular to the longitudinal direction of the sample is that the sample is oriented to some extent.

Figure 8. Temperature dependence of the linear thermal strain of $Ni_{52.7}Mn_{24.3}Ga_{23}$ in static magnetic fields, parallel to the longitudinal direction of the sample.

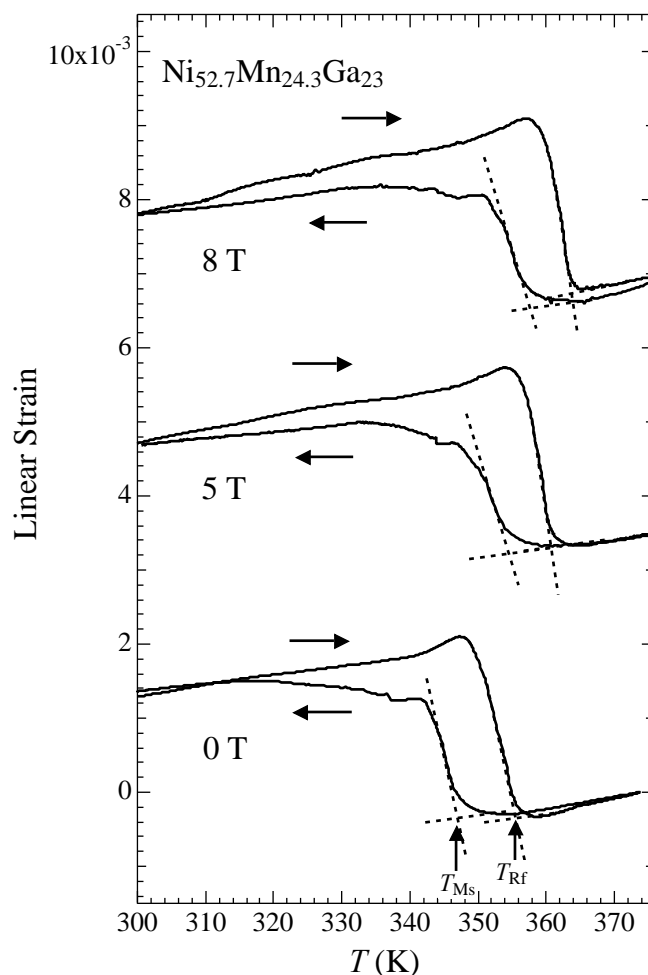
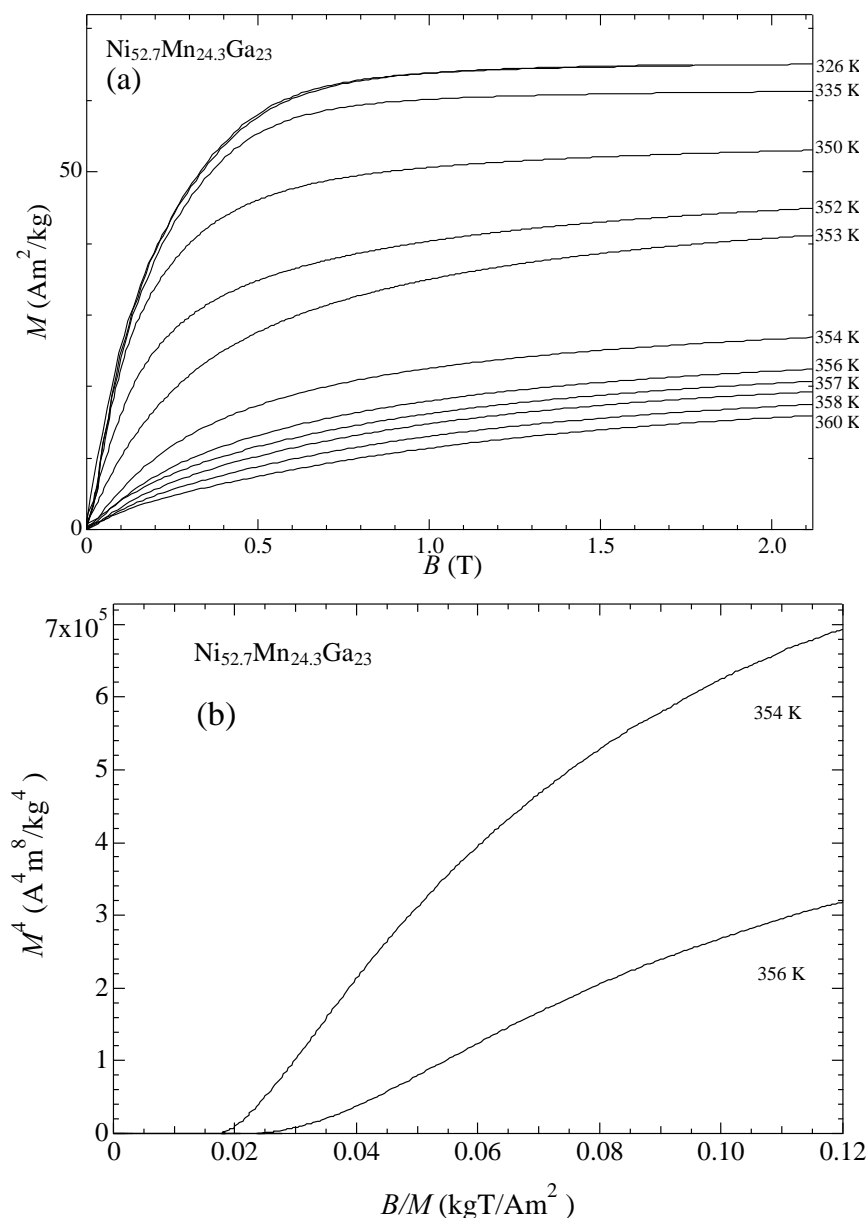


Figure 9a shows the magnetization process of $\text{Ni}_{52.7}\text{Mn}_{24.3}\text{Ga}_{23}$. The experiments were performed in steady fields. This is because that this alloy shows the martensite transition and ferromagnetic transition at the same temperature. Then the latent heat is not small at T_C . In order to avoid heating or cooling due to the ferromagnetic and martensite transition, we measured in steady fields and isothermal processes. The magnetization suddenly changes at $T_C = 356$ K. The spontaneous magnetization change ΔM is $28 \text{ Am}^2/\text{kg}$. The M^4 vs. B/M plot is shown in Figure 9b. This plot did not indicate a linear relation around the Curie temperature. Takahashi's theory can be applied to isotropic ferromagnet. Below $x = 2.5$, T_C is higher than T_M and a ferromagnetic transition occurs in the austenite phase. Between T_M and T_C , the magnetic property is isotropic ferromagnet. On the contrary, $x = 2.7$ transfers from the martensite ferromagnet to the austenite paramagnet. In the martensite phase, magnetic anisotropy is larger than that in the austenite phase. Therefore, it is supposed that Takahashi's theory cannot be applied to $x = 2.7$.

Figure 9. (a) Magnetization of $\text{Ni}_{52.5}\text{Mn}_{24.5}\text{Ga}_{23}$ in a static field; (b) M^4 vs. B/M plot for $\text{Ni}_{52.7}\text{Mn}_{24.5}\text{Ga}_{23}$.



3.3. The Magnetic Field Dependence of the Martensite Transition Temperature

Now we discuss about the field dependence of the martensite transition temperature.

The martensite transition temperature change (dT) induced by magnetic field change (dB) is approximately given by the Clausius-Clapeyron relation [8,32,33]:

$$\frac{dB}{dT} = \frac{\Delta S}{\Delta M} \quad [\text{T/K}] \quad (2)$$

where, ΔS and ΔM are the differences in entropy and magnetization between austenite and martensite phase. The entropy change ΔS was calculated by DSC result.

For $\text{Ni}_{52}\text{Mn}_{25}\text{Ga}_{23}$, the entropy change ΔS due to the martensite transition is 20 J/kg·K. The magnetization change $\Delta M = 11 \text{ Am}^2/\text{kg}$, therefore $\Delta S/\Delta M = 1.8 \text{ T/K}$, and $dT_M/dB = 0.55 \text{ K/T}$. The experimental result of dT_M/dB is $0.43 \pm 0.1 \text{ K/T}$ [24].

For $\text{Ni}_{52.5}\text{Mn}_{24.5}\text{Ga}_{23}$, the entropy change ΔS is 22 J/kg·K. Magnetization change $\Delta M = 17 \text{ Am}^2/\text{kg}$, therefore $\Delta S/\Delta M = 1.3 \text{ T/K}$, and $dT_M/dB = 0.77 \text{ K/T}$. The experimental result of dT_M/dB is $0.9 \pm 0.2 \text{ K/T}$ (this work).

For $\text{Ni}_{52.7}\text{Mn}_{24.3}\text{Ga}_{23}$, the entropy change ΔS is 26 J/kg·K. Magnetization change $\Delta M = 34 \text{ Am}^2/\text{kg}$, therefore $\Delta S/\Delta M = 0.76 \text{ T/K}$, and $dT_M/dB = 1.3 \text{ K/T}$. The experimental result of dT_M/dB is $1.1 \pm 0.2 \text{ K/T}$ (this work). The dT_M/dB 's are approximately as same as that of the calculated values.

Khovailo *et al.* [34,35] discussed the correlation between the shifts in T_M for $\text{Ni}_{2+x}\text{Mn}_{1-x}\text{Ga}$ ($0 \leq x \leq 0.19$) using theoretical calculations according to Clausius-Clapeyron formalism. The experimental values of this shift for $\text{Ni}_{2+x}\text{Mn}_{1-x}\text{Ga}$ ($0 \leq x \leq 0.19$) are in good agreement with the theoretical calculation results. In general, in a magnetic field, the Gibbs free energy is lowered by the Zeeman energy $-\Delta MB$, which enhances the motive force of the martensite phase transition. Thus the T_M 's of the ferromagnetic Heusler alloys are considered to have shifted in accordance with magnetic fields because high magnetic fields are favorable for ferromagnetic martensite phases.

The relationship between magnetism and T_M in magnetic fields is discussed for other Ni_2MnGa -type Heusler alloys. Table 1 shows the spontaneous magnetizations and dT_M/dB values of $\text{Ni}_{2+x}\text{Mn}_{1-x}\text{Ga}$, $\text{Ni}_{52}\text{Mn}_{12.5}\text{Fe}_{12.5}\text{Ga}_{23}$, $\text{Ni}_2\text{Mn}_{0.75}\text{Cu}_{0.25}\text{Ga}$, $\text{Ni}_2\text{MnGa}_{0.88}\text{Cu}_{0.12}$, and $\text{Ni}_{52}\text{Mn}_{25}\text{Ga}_{23}$. As for $\text{Ni}_{2+x}\text{Mn}_{1-x}\text{Ga}$ alloys, shifts in the T_M of the magnetic fields were observed by magnetization measurements [2,34,36,37]. The T_M and T_C of Ni_2MnGa ($x = 0$) are 200 and 360 K, respectively. The region above T_M is the Ferro–A phase. A sample where $x = 0$ for $\text{Ni}_{2+x}\text{Mn}_{1-x}\text{Ga}$ showed a phase transition from the Ferro–A to the Ferro–M phases at T_M . A sample where $x = 0.19$ showed ferromagnetic transition and martensite transition at T_M . When $x = 0$, the shift in T_M was estimated as $dT_M/dB = 0.2 \text{ K/T}$ [20] and where $x = 0.19$, $dT_M/dB = 0.8 \text{ K/T}$ [37]. The shift in T_M where $x = 0.19$ was higher than that for $x = 0$. The last four alloys in Table 1 show re-entrant magnetic transition. In these alloys, ferromagnetic transition occurs at the martensite transition. Below T_M , the paramagnetic martensite phase (Para–M) appears. On the other hand, above T_M , the austenite ferromagnetic phase (Ferro–A) appears. The ground states of these alloys are the ferromagnetic martensite phase at low temperature. Therefore, re-entrant magnetism appears. In a magnetic field, the ferromagnetic phase is more stable than the paramagnetic phase is. Therefore, T_M decreases with increasing magnetic fields while the ferromagnetic phase area

increases; the sign of dT_M/dB is negative. In these alloys, the values of dT_M/dB are large. This means that strong magneto-structural coupling was revealed through magnetic properties and phase transitions.

Table 1. Spontaneous magnetization and dT_M/dB in Heusler Ni_2MnGa type magnetic shape memory alloys. M_M and M_A indicate the spontaneous magnetizations in the martensite phase and austenite phases, respectively. Ferro and Para indicate the ferromagnetic and the paramagnetic phases, respectively. T_C^M indicates the Curie temperature in the martensite phase, and T_C^A indicates the Curie temperature in the austenite phase. The * symbols in this table (eg. *1) indicate the references as shown in Remarks column.

Sample	M_M	M_A	$dT_M/dB(K/T)$	Remarks
Ni_2MnGa	90 Am ² /kg at 180 K (*1) Ferro	80 Am ² /kg at 220 K (*1) Ferro	0.20 (*2) 0.40 ± 0.25 (*3)	*1 [2]; *2 [36]; *3 [37]
$Ni_{2.19}Mn_{0.81}Ga$	2.0 (a.u.) at 300 K Ferro	0 (a.u.) at 350 K Para	0.80 ± 0.5	[34]
$Ni_{52}Mn_{12.5}Fe_{12.5}Ga_{23}$	63.1 Am ² /kg at 250 K Ferro	52.7 Am ² /kg at 300 K Ferro	0.5	[26]
$Ni_2Mn_{0.75}Cu_{0.25}Ga$	42.4 Am ² /kg at 300 K Ferro	0 Am ² /kg at 307 K Para	1.2	[26]
$Ni_2MnGa_{0.88}Cu_{0.12}$	37.3 Am ² /kg at 330 K Ferro	0 Am ² /kg at 340 K Para	1.3	[38]
$Ni_{52}Mn_{25}Ga_{23}$	42 Am ² /kg at 333 K Ferro	34 Am ² /kg at 335 K Ferro	0.43 ± 0.1	[24]
$Ni_{52.5}Mn_{24.5}Ga_{23}$	39 Am ² /kg at 338 K Ferro	22 Am ² /kg at 343 K Ferro	0.9 ± 0.2	this work
$Ni_{52.7}Mn_{24.3}Ga_{23}$	34 Am ² /kg at 352 K Ferro	0 Am ² /kg at 356 K Para	1.1 ± 0.2	this work
$Ni_{45}Co_5Mn_{36.7}In_{13.3}$	0 Am ² /kg at 270 K Para	70 Am ² /kg at 320 K Ferro	-4.3	[33]
$Ni_{43}Co_7Mn_{31}Ga_{19}$	20 Am ² /kg at $T_C^M \leq T \leq T_M$ Para or weak Ferro	59.2 Am ² /kg at $T_M \leq T \leq T_C^A$ Ferro	-2.95	[39]
$Ni_{41}Co_9Mn_{32}Ga_{18}$	4.0 Am ² /kg at $T_C^M \leq T \leq T_M$ Para or weak Ferro	53.3 Am ² /kg at $T_M \leq T \leq T_C^A$ Ferro	-2.8	[39]
$Ni_{41}Co_9Mn_{31.5}Ga_{18.5}$	12 Am ² /kg at $T_C^M \leq T = 316 K \leq T_M$ Para or weak Ferro	79 Am ² /kg at $T_M \leq T = 388 K \leq T_C^A$ Ferro	-4.2	[40]

3.4. Magneto-Structural Coupling of Ni_2MnGa -type Heusler Alloys

Finally, we comment on the $x-T$ phase diagram of Ni_2MnGa -type Heusler alloys. As for the $x-T$ phase diagram of $Ni_{50+x}Mn_{27-x}Ga_{23}$ alloys ($-25 \leq x \leq 6$), the T_M increases with increasing x . In contrast, the T_C decreases with decreasing x . Kataoka *et al.* [41] explained the phase diagram of $Ni_2Mn_{1-x}Cu_xGa$ ($0 \leq x \leq 0.40$) alloys. They conceived of the Landau-type phenomenological free energy as a function of martensitic distortion and magnetization. Their analysis showed that the bi-quadratic coupling term of martensitic distortion and magnetization, together with a higher order term, play an important role in the interplay between the martensite and ferromagnetic phases. Their calculation was based on the phenomenological free energy, shown as:

$$F_{tot} = F_{ela} + F_{mag} + F_{mag-ela} \quad (2)$$

where, F_{tot} is the total free energy; F_{ela} , the free energy of the elastic strain e_{ij} ; F_{mag} , the free energy of the magnetic system (including the magnetic exchange energy and the magnetocrystalline anisotropy energy) and $F_{mag-ela}$, the energy of the interaction between the distortion and the magnetization. The calculated $x-T$ phase diagram of $Ni_2Mn_{1-x}Cu_xGa$ agrees well with the phase diagram, which was

obtained from the experimental results. In addition, using the martensitic distortion coefficient e_3 , they suggested that the bi-quadratic term, $e_3^2 M^2$, in $F_{\text{mag-ela}}$, affects large magneto-structural coupling. ($e_3 = (2e_{zz} - e_{xx} - e_{yy}) / \sqrt{6}$, where, e_{xx} , e_{yy} and e_{zz} are strains along x , y , and z axis, respectively). Thus, strong magneto-structural coupling was shown to have an important role in the magnetic properties and phase transitions of ferromagnetic shape memory alloys. Large magnetocrystalline anisotropy influences magneto-elastic coupling $F_{\text{mag-ela}}$ by means of the bi-quadratic term, $e_3^2 M^2$. In $\text{Ni}_{50-x}\text{Co}_x\text{Mn}_{31.5}\text{Ga}_{18.5}$ ($0 \leq x \leq 9$), magnetization M increases with the magnetic field between 338 K and 388 K [40]. The thermal hysteresis of the thermal strain also decreases at high magnetic fields. Other Heusler compounds, such as $\text{Ni}_{50+x}\text{Mn}_{12.5}\text{Fe}_{12.5}\text{Ga}_{25-x}$, show an x - T phase diagram similar to that of $\text{Ni}_2\text{Mn}_{1-x}\text{Cu}_x\text{Ga}$ [26]. The magnetic field-induced strain in single crystals, or magnetostriction in polycrystals, of Ni_2MnGa , Ni-Co-Mn-Ga , and Ni-Co-Mn-In alloys also suggest a strong magneto-structural coupling. The x - T phase diagram of $\text{Ni}_{50+x}\text{Mn}_{27-x}\text{Ga}_{23}$ alloys ($-25 \leq x \leq 6$) also shows the same characters as that of $\text{Ni}_2\text{Mn}_{1-x}\text{Cu}_x\text{Ga}$ ($0 \leq x \leq 0.40$) alloys [19]. The x - T phase diagram of $\text{Ni}_{50+x}\text{Mn}_{27-x}\text{Ga}_{23}$ indicates a strong magneto-structural coupling for $\text{Ni}_{50+x}\text{Mn}_{27-x}\text{Ga}_{23}$ alloys.

To apply this theory to our present work, further theoretical consideration is needed to apply this theory for analyzing the relationship between the martensite variant structure and the magnetic field, which is reflected by the Zeeman term, and Jahn-Teller effect, which is applied to the ferrites and perovskite compounds [42,43].

4. Conclusions

Thermal strain, permeability, and magnetization measurements were performed on the Heusler alloys $\text{Ni}_{52.5}\text{Mn}_{24.5}\text{Ga}_{23}$ ($x = 2.5$) and $\text{Ni}_{52.7}\text{Mn}_{24.3}\text{Ga}_{23}$ ($x = 2.7$).

1. Thermal strain: When cooling from the austenite phase, a steep decrease in the thermal strain was obtained because of the martensite transition. T_M and T_R increased gradually with increasing magnetic fields. For $x = 2.5$, The shift in T_M in the magnetic field was estimated as $dT_{M_s}/dB = 0.9 \pm 0.2$ K/T. For $x = 2.7$, the shift in T_M in the magnetic field was estimated as $dT_{M_s}/dB = 1.1 \pm 0.2$ K/T.
2. The dT_{M_s}/dB values determined from the thermal strain results are approximately as same as the values calculated by the Clausius-Clapeyron relation.
3. For $x = 2.5$, at the Curie temperature, the M^4 vs. B/M plot crossed the origin of the coordinate axis, and the M^4 vs. B/M plot indicates a good linear relation around the Curie temperature $T_C = 350$ K. The result is in agreement with the theory by Takahashi for weak itinerant electron ferromagnets. From the magnetic moment and the gradient of M^4 vs. B/M , we calculated the spin fluctuation parameter T_A as 1.06×10^4 K, which is comparable to the value of Ni (1.76×10^4 K).

Acknowledgments

The authors would like to express sincere thanks to Toetsu Shishido and Kazuo Obara of the Institute for Materials Research, Tohoku University for their help with the sample preparation. This study was supported by a Grant-in-Aid for Scientific Research (C) (Grant No. 21560693) from the

Japan Society for the Promotion of Science (JSPS) of the Ministry of Education, Culture, Sports, Science and Technology, Japan.

This study was technically supported by the Center for Integrated Nanotechnology Support, Tohoku University, and the High Field Laboratory for Superconducting Materials, Institute for Materials Research, Tohoku University. One of the authors, Hiroyuki Nojiri, acknowledges support by GCOE-material integration.

Author Contributions

Takuo Sakon designed, directed, carried out the experiments and wrote the paper, Kohei Otsuka carried out the DSC measurements, Junpei Matsubayashi carried out the permeability and magnetization measurements by means of helium-free magnet, Yuushi Watanabe carried out the thermal expansion and magnetostriction measurements, Hironori Nishihara carried out the magnetization measurements by means of SQUID magnetometer, Kenta Sasaki carried out the thermal expansion and magnetostriction measurements, Satoshi Yamashita, Rie Y. Umetsu, and Takeshi Kanomata made and homogenized the samples. Hiroyuki Nojiri supported this experimental project at IMR, Tohoku University, Takeshi Kanomata also advised about the scientific meanings of this study and edited the paper.

Conflicts of Interest

The authors declare no conflict of interest.

References

1. Ullakko, K.; Huang, J.K.; Kantner, C.; O'Handley, R.C.; Kokorin, V.V. Large magnetic-field-induced strains in Ni₂MnGa single crystals. *Appl. Phys. Lett.* **1996**, *69*, 1966–1968.
2. Webster, P.J.; Ziebeck, K.R.A.; Town, S.L.; Peak, M.S. Magnetic order and phase transformation in Ni₂MnGa. *Philos. Mag. B* **1984**, *49*, 295–310.
3. Brown, P.J.; Crangle, J.; Kanomata, T.; Matsumoto, M.; Neumann, K.-U.; Ouladdiaf, B.; Ziebeck, K.R.A. The crystal structure and phase transitions of the magnetic shape memory compound Ni₂MnGa. *J. Phys. Condens. Matter* **2002**, *14*, 10159–10171.
4. Pons, J.; Santamarta, R.; Chernenko, V.A.; Cesari, E. Long-Period martensitic structures of Ni-Mn-Ga alloys studied by high-resolution transmission electron microscopy. *J. Appl. Phys.* **2005**, *97*, 083516:1–083516:7.
5. Ranjan, R.; Banik, S.; Barman, S.R.; Kumar, U.; Mukhopadhyay, P.K.; Pandey, D. Powder X-ray diffraction study of the thermoelastic martensite transition in Ni₂Mn_{1.05}Ga_{0.95}. *Phys. Rev. B* **2006**, *74*, 224443:1–224443:2.
6. Jiang, C.; Feng, G.; Gong, S.; Xu, H. Effect of Ni excess on phase transformation temperatures of NiMnGa alloys. *Mater. Sci. Eng. A* **2003**, *342*, 231–235.
7. Ma, Y.; Jiang, C.; Li, Y.; Xu, H.; Wang, C.; Liu, X. Study of Ni_{50+x}Mn₂₅Ga_{25-x} ($x = 2-11$) as high-temperature shape-memory alloys. *Acta Mater.* **2007**, *55*, 1533–1541.

8. Mañosa, L.; Moya, X.; Planes, A.; Krenke, T.; Acet, M.; Wassermann, E.F. Ni-Mn-based magnetic shape memory alloys: Magnetic properties and martensite transformation. *Mater. Sci. Eng. A* **2008**, *481–482*, 49–56.
9. Sánchez-Alarcos, V.; Pérez-Landazábal, J.I.; Gómez-Polo, C.; Recarte, V. Influence of the atomic order on the magnetic characteristics of a Ni-Mn-Ga ferromagnetic shape memory alloy. *J. Magn. Magn. Mater.* **2008**, *320*, e160–e163.
10. Rudajevová, A. Analysis of the thermal expansion characteristics of Ni_{53.6}Mn_{27.1}Ga_{19.3} alloy. *J. Alloys Compd.* **2007**, *430*, 153–157.
11. Zhu, F.Q.; Yang, F.Y.; Chien, C.L.; Ritchie, L.; Xiao, G.; Wu, G.H. Magnetic and thermal properties of Ni–Mn–Ga shape memory alloy with Martensite transition near room temperature. *J. Magn. Magn. Mater.* **2005**, *288*, 79–83.
12. Chernenko, V.A.; L'vov, V.A.; Khovailo, V.V.; Takagi, T.; Kanomata, T.; Suzuki, T.; Kainuma, R. Interdependence between the magnetic properties and lattice parameters of Ni-Mn-Ga martensite. *J. Phys. Condens. Matter* **2004**, *16*, 8345–8352.
13. Golub, V.O.; Vovk, A.Y.; O'Connor, C.J.; Kotov, V.V.; Yakovenko, P.G.; Ullakko, K. Magnetic and structural properties of nonstoichiometric Ni₂MnGa alloys with Ni and Ga excess. *J. Appl. Phys.* **2003**, *93*, 8504–8506.
14. Kim, J.; Inaba, F.; Fukuda, T.; Kakeshita, T. Effect of magnetic field on martensitic transformation temperature in Ni-Mn-Ga ferromagnetic shape memory alloys. *Acta Mater.* **2006**, *54*, 493–499.
15. González-Comas, A.; Obradó, E.; Mañosa, L.; Planes, A.; Labarta, A. Magnetoelasticity in the Heusler Ni₂MnGa alloy. *J. Magn. Magn. Mater.* **1999**, *196–197*, 637–638.
16. Lanska, N.; Söderberg, O.; Sozinov, A.; Ge, Y.; Ullakko, K.; Lindroos, V.K. Composition and temperature dependence of the crystal structure of Ni-Mn-Ga alloys. *J. Appl. Phys.* **2004**, *95*, 8074–8078.
17. Likhachev, A.A.; Ullakko, K. Magnetic-field-controlled twin boundaries motion and giant magneto-mechanical effects in Ni-Mn-Ga shape memory alloy. *Phys. Lett. A* **2000**, *275*, 142–151.
18. Murray, S.J.; Farinelli, M.; Kantner, C.; Huang, J.K.; Allen, S.M.; O'Handley, R.C. Field-induced strain under load in Ni-Mn-Ga magnetic shape memory materials. *J. Appl. Phys.* **1998**, *83*, 7297–7299.
19. Umetsu, R.Y.; Ando, H.; Yamashita, S.; Endo, K.; Nishihara, H.; Kainuma, R.; Kanomata, T.; Ziebeck, K.R.A. Phase diagram and magnetic moment of Ni_{50+x}Mn_{27-x}Ga₂₃ ferromagnetic shape memory alloys. *J. Alloys Compd.* **2013**, *579*, 521–528.
20. Dai, L.; Cullen, J.; Wuttig, M. Intermartensitic transformation in a NiMnGa alloy. *J. Appl. Phys.* **2004**, *95*, 6957–6959.
21. Takahashi, Y. Quantum spin fluctuation theory of the magnetic equation of state of weak itinerant-electron ferromagnets. *J. Phys. Condens. Matter* **2001**, *13*, 6323–6358.
22. Takahashi, Y. *Spin Fluctuation Theory of Itinerant Electron Magnetism*; Springer-Verlag: Berlin/Heidelberg, Germany, 2013.
23. Nishihara, H.; Komiyama, K.; Oguro, I.; Kanomata, T.; Chernenko, V.; Magnetization processes near the Curie temperatures of the itinerant ferromagnets, Ni₂MnGa and pure nickel. *J. Alloys Compd.* **2007**, *442*, 191–193.

24. Sakon, T.; Nagashio, H.; Sasaki, K.; Susuga, S.; Numakura, D.; Abe, M.; Endo, K.; Yamashita, S.; Nojiri, H.; Kanomata, T. Thermal strain and magnetization of the ferromagnetic shape memory alloy $\text{Ni}_{52}\text{Mn}_{25}\text{Ga}_{23}$ in a magnetic field. *J. Phys. Chem. Solids* **2013**, *74*, 158–165.
25. Kikuchi, D.; Kanomata, T.; Yamaguchi, Y.; Nishihara, H. Magnetic properties of ferromagnetic shape memory alloys $\text{Ni}_{50+x}\text{Mn}_{12.5}\text{Fe}_{12.5}\text{Ga}_{25-x}$. *J. Alloys Compd.* **2006**, *426*, 223–227.
26. Sakon, T.; Nagashio, H.; Sasaki, K.; Susuga, S.; Endo, K.; Nojiri, H.; Kanomata, T. Thermal expansion and magnetization studies of novel ferromagnetic shape memory alloys $\text{Ni}_{52}\text{Mn}_{12.5}\text{Fe}_{12.5}\text{Ga}_{23}$ and $\text{Ni}_2\text{Mn}_{0.75}\text{Cu}_{0.25}\text{Ga}$. *Mater. Trans.* **2011**, *52*, 1142–1147.
27. Okamoto, N.; Fukuda, T.; Kakeshita, T.; Takeuchi, T. Magnetocrystalline anisotropy constant and twinning stress in martensite phase of Ni-Mn-Ga. *Mater. Sci. Eng. A* **2006**, *438–440*, 948–951.
28. Ahuja, B.L.; Sharma, B.K.; Mathur, S.; Heda, N.L.; Itou, M.; Andrejczuk, A.; Sakurai, Y.; Chakrabarti, A.; Banik, S.; Awasthi, A.M.; *et al.* Magnetic Compton scattering study of $\text{Ni}_{2+x}\text{Mn}_{1-x}\text{Ga}$ ferromagnetic shape-memory alloys. *Phys. Rev. B* **2007**, *75*, 134403:1–134403:9.
29. Levitin, R.Z.; Snegirev, V.V.; Kopylov, A.V.; Lagutin, A.S.; Gerber, A. Magnetic method of magnetocaloric effect determination in high pulsed magnetic fields. *J. Magn. Magn. Mater.* **1997**, *170*, 223–227.
30. Nishihara, H.; Furutani, Y.; Wada, T.; Kanomata, T.; Kobayashi, K.; Kainuma, R.; Ishida, K.; Yamauchi, T. Magnetization process near the curie temperature of a ferromagnetic heusler alloy Co_2CrGa . *J. Phys. Conf. Ser.* **2007**, *200*, 032053:1–032053:4.
31. Vasil'ev, A.N.; Estrin, E.I.; Khovailo, V.V.; Bozhko, A.D.; Ischuk, R.A.; Matsumoto, M.; Takagi, T.; Tani, J. Dilatometric study of $\text{Ni}_{2+x}\text{Mn}_{1-x}\text{Ga}$ under magnetic field. *Int. Appl. Electromagn. Mech.* **2000**, *12*, 35–40.
32. Banerjee, A.; Dash, S.; Lakhani, A.; Chaddah, P.; Chen, X.; Ramanujan, R.V. Relating field-induced shift in transition temperature to the kinetics of coexisting phases in magnetic shape memory alloys. *Solid State Commun.* **2011**, *151*, 971–975.
33. Kainuma, R.; Imano, Y.; Ito, W.; Sutou, Y.; Morino, H.; Okamoto, S.; Kitakami, O.; Oikawa, K.; Fujita, A.; Kanomata, T.; *et al.* Magnetic-field-induced shape recovery by reverse phase transformation. *Nature* **2006**, *439*, 957–960.
34. Khovailo, V.V.; Novosad, V.; Takagi, T.; Filippov, D.A.; Levintin, R.Z.; Vasil'ev, A.N.; Magnetic properties and magnetostructural phase transitions in $\text{Ni}_{2+x}\text{Mn}_{1-x}\text{Ga}$ shape memory alloys. *Phys. Rev. B* **2004**, *70*, 174413–174418.
35. Khovailo, V.V.; Takagi, T.; Tani, T.J.; Levitin, R.Z.; Cherechukin, A.A.; Matsumoto, M.; Note, R. Magnetic properties of $\text{Ni}_{2.18}\text{Mn}_{0.82}\text{Ga}$ Heusler alloys with a coupled magnetostructural transition. *Phys. Rev. B* **2002**, *65*, 092410–092413.
36. González-Comas, A.; Obradó, E.; Maños, L.; Planes, A.; Chernenko, V.A.; Hattink, B.J.; Labarta, A. Premartensitic and martensitic phase transitions in ferromagnetic Ni_2MnGa . *Phys. Rev. B* **1999**, *60*, 7085–7090.
37. Filippov, D.A.; Khovailo, V.V.; Koledov, V.V.; Krasnoperov, E.P.; Levitin, R.Z.; Shavrov, V.G.; Takagi, T. The magnetic field influence on magnetostructural phase transition in $\text{Ni}_{2.19}\text{Mn}_{0.81}\text{Ga}$. *J. Magn. Magn. Mater.* **2003**, *258–259*, 507–509.

38. Sakon, T.; Nagashio, H.; Sasaki, K.; Susuga, S.; Numakura, D.; Abe, M.; Endo, K.; Nojiri, H.; Kanomata, T. Thermal expansion and magnetization studies of the novel ferromagnetic shape memory alloy $\text{Ni}_2\text{MnGa}_{0.88}\text{Cu}_{0.12}$ in a magnetic field. *Phys. Scr.* **2011**, *84*, 045603:1–045603:6.
39. Albertini, F.; Fabbri, S.; Paoluzi, A.; Kamarad, J.; Arnold, Z.; Righi, L.; Solzi, M.; Porcari, G.; Pernechele, C.; Serrate, D.; *et al.* Reverse magnetostructural transitions by Co and In doping NiMnGa alloys: Structural, magnetic, and magnetoelastic properties. *Mater. Sci. Forum* **2011**, *684*, 151–163.
40. Sakon, T.; Sasaki, K.; Numakura, D.; Abe, M.; Nojiri, H.; Adachi, Y.; Kanomata, T. Magnetic field-induced transition in Co-doped $\text{Ni}_{41}\text{Co}_9\text{Mn}_{31.5}\text{Ga}_{18.5}$ Heusler Alloy. *Mater. Trans.* **2013**, *54*, 9–13.
41. Kataoka, M.; Endo, K.; Kudo, N.; Kanomata, T.; Nishihara, H.; Shishido, T.; Umetsu, R.Y.; Nagasako, M.; Kainuma, R. Martensitic transformation, ferromagnetic transition, and their interplay in the shape memory alloys $\text{Ni}_2\text{Mn}_{1-x}\text{Cu}_x\text{Ga}$. *Phys. Rev. B* **2010**, *82*, 214423:1–214423:14.
42. Kataoka, M.; Kanamori, J. A theory of the cooperative Jahn-Teller effect-crystal distortions in $\text{Cu}_{1-x}\text{Ni}_x\text{Cr}_2\text{O}_4$ and $\text{Fe}_{1-x}\text{Ni}_x\text{Cr}_2\text{O}$. *J. Phys. Soc. Jpn.* **1972**, *32*, 113–134.
43. Gehring, G.A.; Gehring, K.A. Cooperative Jahn-Teller effects. *Rep. Prog. Phys.* **1975**, *38*, 1–89.

© 2014 by the authors; licensee MDPI, Basel, Switzerland. This article is an open access article distributed under the terms and conditions of the Creative Commons Attribution license (<http://creativecommons.org/licenses/by/3.0/>).